Available online at www.sciencedirect.com
ScienceDirect
Bioorganic & Medicinal Chemistry 15 (2007) 2081–2091
Bioorganic & Medicinal Chemistry

1,4-Bis(alkylamino)benzo[*g*]phthalazines able to form dinuclear complexes of Cu(II) which as free ligands behave as SOD inhibitors and show efficient in vitro activity against *Trypanosoma cruzi*

Marinela Rodríguez-Ciria,[a] Ana M. Sanz,[a] María J. R. Yunta,[a] Fernando Gómez-Contreras,[a,*] Pilar Navarro,[b] Manuel Sánchez-Moreno,[c,*] Samira Boutaleb-Charki,[c] Antonio Osuna,[c] Alfonso Castiñeiras,[d] Mercedes Pardo,[a] Carmen Cano[a] and Lucrecia Campayo[a]

[a]*Departamento de Química Orgánica I, Facultad de Química, Universidad Complutense, 28040 Madrid, Spain*
[b]*Instituto de Química Medica, Centro de Química Orgánica Manuel Lora-Tamayo, CSIC, Juan de la Cierva, 3, 28006 Madrid, Spain*
[c]*Instituto de Biotecnología, Facultad de Ciencias, Universidad de Granada, 18071 Granada, Spain*
[d]*Departamento de Química Inorgánica, Facultad de Farmacia, Universidad de Santiago, 15782 Santiago de Compostela, Spain*

Received 1 September 2006; revised 12 December 2006; accepted 20 December 2006
Available online 23 December 2006

Abstract—The synthesis of a new series of 1,4-bis(alkylamino)benzo[*g*]phthalazines **1**–**3** is reported, and their ability to form dinuclear complexes with Cu(II) assayed. The geometry of the complexes is dependent on the nature of the electron-donor sites at the sidechains. Compounds **1** and **2**, that contain sp^3 or sp^2 nitrogens at the end of the alkylamino groups, originate monopodal dinuclear complexes which seem to include endogenous OH bridges, and the sidechains seem to actively participate in complexation. However, the substitution of nitrogen by oxygen in **3** leads to a tripodal dinuclear complex in which the sidechains are not involved. The in vitro antiparasitic activity on *Trypanosoma cruzi* epimastigotes and amastigotes and the SOD activity inhibition have been evaluated for compounds **1**–**3**, and, as expected, **1** and **2** show in all cases relevant results, whereas **3** is always the less active among the three substrates tested.

1. Introduction

Parasitic diseases represent an increasing threat to human health. Leishmaniasis and Chagas disease are major causes of mortality in tropical areas, and account for more than one million deaths a year.[1,2] Chagas disease, produced by protozoan parasite of the order *Trypanosoma cruzi*,[3] is endemic in 21 countries, and it has been calculated that, only in Central and South America, about 18 millions of people are infected and 100 millions are on risk.[4] Currently available chemotherapy is unsatisfactory because of its limited efficacy in the prevalent chronic stage of the disease ant toxic side effects.[3] However, the last years have witnessed an impressive increase in our understanding of the biochemistry and molecular biology of parasites, so that a major challenge is present for developing new antiparasitic drugs on the basis of that knowledge.

It has been shown that, in general, parasitic protozoan survival is closely related to the ability of enzymes for evading toxic free radical damage originated by their host.[5] One of these mechanisms involves superoxide dismutases (SOD). It seems that these enzymes act as scavengers that protect trypanosomatides like *Leishmania tropica* and *T. cruzi* from the damning effects of the superoxide anions or hydroxyl radicals produced in O_2 reduction.[6,7] It has been suggested that an increase in superoxide due to the inhibition of SOD would affect both the growth and survival of parasited cells.

Three distinct types of SOD have been isolated from various species of organisms, and each of them contains

Keywords: 1,4-Bis(alkylamino)benzo[*g*]phthalazines; *Trypanosoma cruzi* SOD inhibitors; Dinuclear copper complexes; OH endogenous bridges; Antiparasitic activity.
* Corresponding authors. Fax: +34913944103; e-mail: fercon@quim.ucm.es

0968-0896/$ - see front matter © 2007 Elsevier Ltd. All rights reserved.
doi:10.1016/j.bmc.2006.12.033

different transition metals as the prosthetic group: Cu/Zn, Fe and Mn. The metal ligands are in all cases aminoacid residues, varying in composition according to the type of species or even subspecies considered. Maybe the most widely present in different organisms is the homodimeric CuZnSOD, usually containing one copper and one zinc ion bridged by imidazolate and bound to imidazole units from histidines.[8] However, it has been shown that only the copper ion is essential for achieving catalysis, since the species E_2Zn_2SOD is completely inactive, whereas Cu_2E_2SOD presents an activity only slightly lower than that one of the native enzyme.[9]

Our hypothesis is that molecules with a high ability for the complexation of transition metal ions could compete with SOD for them and would inhibit the protective action of the enzyme, favouring the cell death and assuming an antiparasitic activity.[10] In consequence, and taking into account the ability shown by 1,4-disubstituted phthalazines for the complexation of metallic cations like Cu(II), Co(II), or Zn(II),[11] we have designed a new series of benzo[*g*]phthalazine derivatives with two flexible sidechains containing nitrogen and oxygen atoms as shown in Figure 1. The pyridazine nitrogens should behave as active sites for interacting with the metallic cations, and the presence of the four electronegative centres in the polyaminic sidechains linked by two or three carbon atoms should allow the simultaneous complexation with two ions.

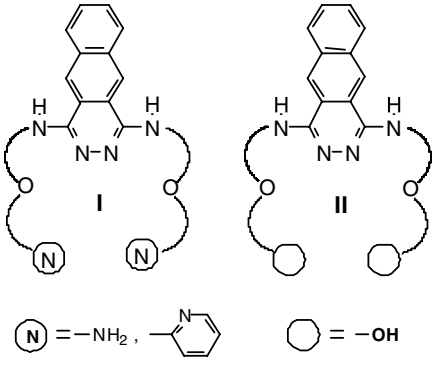

Figure 1.

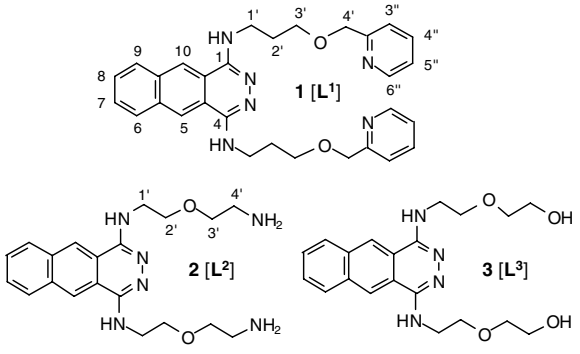

Figure 2.

Moreover, we have systematically modified the nature of the complexation sites located at the end of the aliphatic chains (Fig. 2). So, podands **1** and **2**, containing, respectively, sp^2 (pyridine) and sp^3 (NH_2) nitrogens, were prepared in a first step. In order to evaluate the role of those terminal groups in complexation, we have designed further a third podand, functionalized at the end with OH groups (**3**). In this work, we describe the synthesis of compounds **1**–**3**, their ability for complexing Cu(II) as a model for transition metal ions, and also their parasitic activity against *T. cruzi* and the inhibition of superoxide dismutase.

2. Results and discussion

The preparation of compounds **1**–**3** was performed according to the methodology shown in Scheme 1. Nucleophilic substitution of the starting 1,4-dichlorobenzo[*g*]phthalazine with 3-(2-pyridilmethoxy)propylamine, 2-(2-aminoethoxy)ethylamine, or 2-(2-aminoethoxy)ethanol under 1–2 h reflux of xylene afforded the respective mixtures of the 1,4-bisalkylaminobenzo[*g*]phthalazines **1**–**3** and their monoalkylamino substituted analogues **4**–**6**. Conditions selected corresponded to a modification of the classic method of Körmendy[12] devised by our group.[13] Among a wide range of solvents assayed, xylene showed to be determinant in obtaining better comparative yields of compounds **1**–**3**. The mixtures of mono- and di-substituted products were carefully separated in every case by flash column chromatography and isolated as yellow solids or oils in yields ranging from 25% to 45%.

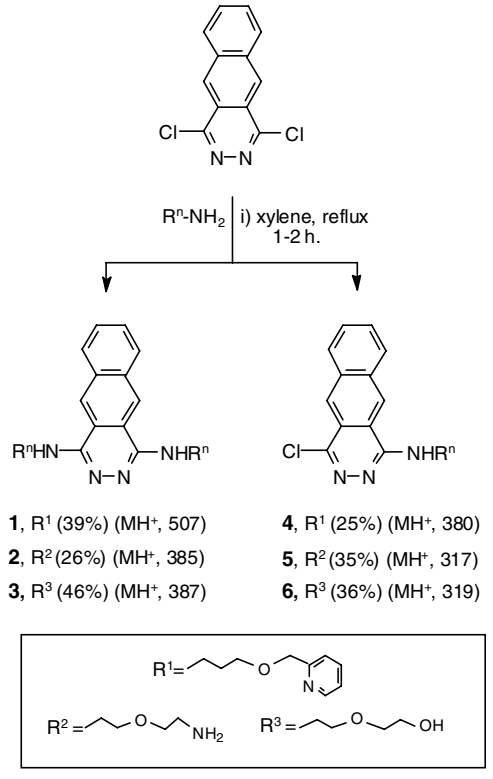

Scheme 1.

The amine required for the preparation of **1** is not commercially available, and was prepared by the reaction of 2-hydroxymethylpyridine with sodium hydride and further treatment of the alkoxide with *N*-(3-bromopropyl)phthalimide. Hydrolysis of the imide with hydrazine in methanol afforded the desired 3-(2-pyridilmethoxy)propylamine in 50% whole yield. It should also be noted that compound **1** was initially obtained in the hydrochloride form, and the free compound was liberated by passing through a basic aluminium oxide column chromatography using chloroform as the eluent.

All the new compounds synthesized were unequivocally identified by their analytical and IR, FAB MS, ^{1}H NMR and ^{13}C NMR spectroscopic data, as shown in Section 4. Scheme 1 displays the molecular ions obtained from the mass spectra of **1**–**6**, which agree in all cases with the proposed structures.

The mono- and diaminoalkyl substitution products are easily differentiated in both ^{1}H and ^{13}C NMR spectra on the basis of signals corresponding to rings A and B of the polyheterocyclic moiety (Table 1). Protons H_5 and H_{10}, which appear as an unique singlet in **1**–**3**, lose their equivalence in their monosubstituted analogues, their chemical shifts differing in about 0.2 ppm in the ^{1}H NMR spectra and 9 ppm in the ^{13}C analogues. Furthermore, the amino substituted carbons are clearly more deshielded than those ones linked to chlorine atoms in the ^{13}C NMR spectra.

The vigorous stirring of a methanol solution of ligands **1**–**3** in the presence of copper(II) perchlorate hexahydrate at room temperature (molar ratio 1:2) led to the formation of green precipitates that were isolated as stable solids in the cases of ligands **1** and **2** (**7** and **8**, respectively) and a highly hygroscopic compound from **3** (**9**), and were identified as the desired complexes. Analytical data for the complex **7** (mp 200–205 °C, 74% yield) gave a formula $C_{31}H_{38}Cl_2Cu_2N_6O_{13}$, that tentatively fitted to $\{[Cu_2\ L^1]\cdot(OH)_2\cdot(ClO_4)_2\cdot MeOH\}$. For complex **8** (mp >300 °C, 39% yield) the formula $C_{20}H_{33}Cl_3Cu_2N_6O_{17}$ was obtained, that corresponded to $\{[Cu_2\ L^2]\cdot(OH)\cdot(ClO_4)_3\cdot(H_2O)_2\}$, and complex **9** (10% yield) afforded $C_{62}H_{86}Cl_4Cu_2N_{12}O_{30}$ assigned to $\{[Cu_2(L^3)_3]\cdot(ClO_4)_4\cdot(MeOH)_2\}$.

The formulae proposed from elemental analysis were confirmed by the FAB mass spectral data. Results obtained show that the complexes of ligands **1** and **2**, which have chain ends containing sp^2 or sp^3 nitrogen atoms, include two copper ions for one ligand unit in both cases, as desired. The fragmentation sequences confirm the presence of perchlorate ions, water molecules and/or hydroxyl groups and indicate the order in which all of them are lost.

The mass spectrum of the complex **7** presents a molecular ion peak MH^+ $m/z = 901$ corresponding to one ligand, two copper ions, two hydroxyl groups, two perchlorate units and one molecule of methanol. The

Table 1. Comparison of the most significant ^{1}H and ^{13}C NMR (δ, CD_3OD, ppm) data for the mono- (**4**–**6**) and bis-alkylamino substituted (**1**–**3**) derivatives

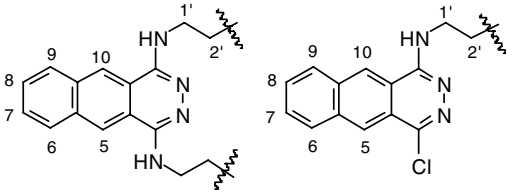

Compound	1	4	2	5	3	6
H_5 (s)	8.55	8.36	8.59	8.48	8.59	8.28
H_{10} (s)	8.55	8.47	8.59	8.64	8.59	8.46
H_6 (m)	7.98	7.96[a]	8.05	8.05	8.05	7.91
H_9 (m)	7.98	7.87[a]	8.05	8.05	8.05	7.91
H_7 (m)	7.65	7.59	7.62	7.66	7.61	7.58
H_8 (m)	7.65	7.59	7.62	7.66	7.61	7.58
$H_{1'}$ (s)	3.66	3.67	3.56	3.58	3.63	3.65
$H_{2'}$ (m)	2.12	2.10	3.81[b]	3.81	3.72[b]	3.73[b]
C_1	150.9	155.6	151.3	155.4	151.3	155.9
C_4	150.9	146.4	151.3	146.2	151.3	146.8
C_{4a}	119.9	123.8	120.0	123.3	120.0	123.9
C_{10a}	119.9	119.4	120.0	118.8	120.0	119.4
C_5	123.4	126.8	123.8	126.1	123.8	126.7
C_{10}	123.4	124.5	123.8	123.8	123.8	124.5
$C_{1'}$	40.6	40.9	43.1	42.7	43.2	43.4
$C_{2'}$	30.1	30.0	70.2	70.0	70.9	70.5

[a] Interchangeable signals.
[b] Triplet.

fragmentation pattern shows initial loss of methanol, followed by two successive losses of perchlorate, the two hydroxyl groups and, finally, the copper ions to give the protonated ligand peak. In a similar way, **8** has a MH^+ $m/z = 865$ fitting to one ligand, two copper units, three perchlorates, one hydroxyl group and two water molecules and exhibits two successive losses of perchlorate, followed by the hydroxyl and water units, the third perchlorate and the two copper ions. All these data not only confirm the proposed molecular formulae but also suggest that the water molecules and/or hydroxyl groups are linked to the copper ions and not located in the outer coordination sphere.

Although we could not dispose of the adequate crystals for performing X-ray diffraction analyses, the geometries of the copper complexes **7** and **8** have been studied by means of a suite of complementary techniques such as IR, electronic and EPR spectroscopies, thermal analysis by pyrolitic decomposition and magnetic susceptibility measures.

The electronic spectra of both compounds (Table 2) exhibit broad bands at, respectively, 648 and 663 nm that are indicative of Cu(II) d–d transitions and suggest the presence of CuN_2O_3 chromophores with a square-pyramidal coordination geometry.[14] This assert is supported by the EPR spectra of both compounds, that show very neat nuclear spin coupling. Hyperfine coupling constant values in the parallel region $A_{\|}$ are estimated as 140 (**7**) and 171 G (**8**), quite similar to the calculated values for D_4 symmetry in each metal atom. Calculated values for $g_{\|} = 2.28$ and $g_{\perp} = 2.05$ in **7** or $g_{\|} = 2.25$ and $g_{\perp} = 2.02$ in **8** are compatible with elongated octahedral or square-based pyramidal geometries with Cu(II) atoms showing interaction in the fundamental $d_{x^2-y^2}$ state with a weak but significant coupling ($G < 4.0$).[15]

On the other hand, the IR spectra of **7** and **8** show that the perchlorate ions are not coordinated to the metal ions. It is known that when ClO_4^- groups are located in a metal complex as ions with Td point symmetry, they have four normal modes of vibration, whereas coordination leads to C_{3v} or C_{2v} point symmetries and rise to nine frequencies of vibration.[16] As can be seen in Table 3, both **7** and **8** exhibit four bands corresponding to $\nu(ClO_4)$.

Furthermore, the ν(NH) bands of the sidechain terminal nitrogens of **8** are shifted to lower frequencies in the complex with respect to the free ligand, indicating that they are coordinated.[17] The participation of the pyridazine nitrogens is deduced from the shift of the ν(CN) band to higher frequencies. This last behaviour is also found in the case of **7**, and involvement of the pyridine nitrogen is observed on the basis of a similar shift and confirmed from the out- and in-plane pyridine ring deformation bands.

Table 2. Electronic and EPR spectra, and magnetic moment of complexes **7** and **8**

	Electronic spectra λ_{max} (nm)	EPR spectra g values	μ_{eff} (rt) (BM)
7	648	$g_{\|} = 2.28$ $g_{\perp} = 2.05$	0.61
8	663	$g_{\|} = 2.25$ $g_{\perp} = 2.02$	0.81

Table 3. Selected IR spectral data for complexes **7** and **8** and their free ligands (cm^{-1})

	$Cu(ClO_4)_2$	**1**	**7**	**2**	**8**
ν(OH, H_2O)	—	—	3407	—	3526, 3403
ν(NH)	—	—	—	3323	3226
ν(CN)	—	1551	1571	1551	1578
$\nu(ClO_4)$	1136	—	1144	—	1141
	—	—	1121	—	1120
	1105	—	1109	—	1108
	1087	—	1086	—	1088
ν(CuO)	—	—		—	392
ν(CuN)	—	—		—	324

The high frequency region shows bands assignable to coordinated and bridged OH and coordinated water molecules in **8**, and broad bands over 3400 cm^{-1} found in **7** can be attributed to any of both types of oxygen coordination.

Finally, Cu–O and Cu–N bond vibrations can be seen clearly in **8**,[18] whereas they cannot be observed in the IR spectrum of **7** due to overlapping with bands corresponding to the ligand skeleton.

Concerning the thermal analysis, it should be noted that the pyrolitic decomposition of **8** begins only at 190 °C, confirming that the water molecules and the hydroxyl ion must be coordinated. The loss of the perchlorate ions occurs at 250 °C and is followed by the elimination of CO_2, H_2O, CO, hydrocyanic, and isocyanic acids to give a residue of CuO. However, **7** begins to lose water between 40 and 200 °C, and this can be attributed to a condensation of the OH ligands forming an oxo bridge and losing water. Methanol is also liberated at low temperatures (40–70 °C). Further behaviour is similar to that commented for **8**.

Last, magnetic susceptibility essays performed in the 5–300 K range showed antiferromagnetic exchange between the copper atoms, supporting the existence of endogenous OH bridges.[19] This is more clearly seen in the case of **8**, with a $-2J$ value of 165.25 cm^{-1} that allows to calculate a Cu(OH)Cu angle of 100° and a Cu–Cu distance of 3.2 Å fitting for seven-membered nitrogen chelates. The magnetic moment at rt is of 0.81 BM. This value is lower in complex **7**, in which 0.61 BM was obtained.

On the basis of all the evidence compiled in the previous paragraphs, we think that the structures of both **7** and **8** could be tentatively assigned as shown in Figure 3. In the two dinuclear complexes the copper atoms appear as pentacoordinated and should adopt a square pyramidal geometry.[15] In complex **7**, each metallic ion should interact with two sp^2 nitrogens from the pyridine and

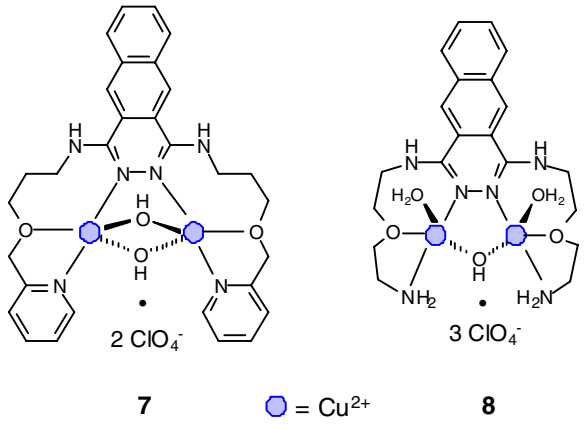

Figure 3.

pyridazine rings and one oxygen atom belonging to the sidechain, and should exhibit two endogenous bridges through hydroxyl groups. That kind of double bridging has been found in a variety of dinuclear copper complexes of nitrogenated heterocycles.[20]

Complex **8** seems to interact in the same way with the ligand, if we change the pyridine sp^2 nitrogen by the sp^3 of the primary amino group. An endogenous OH bridge should also connect the two copper atoms, and the second hydroxo bridge should be replaced by two water molecules, as has been described for benzimidazole and oxazole derivatives,[21] and proposed for the active site of oxyhaemocyanin.[22]

Concerning to the copper complex **9**, formed from ligand **3**, in which the terminal nitrogens have been replaced by OH groups, elemental analysis indicates the presence of three ligand units and two copper ions, in striking contrast to the dinuclear complexes found for ligands **1** and **2** (see Fig. 4). That kind of arrangement has been previously reported for Cu(II) complexes with pyridazine units.[23] The FAB mass spectrum is in accordance with that, because it shows a MH^+ at a very high *m*/*z* 1748, that corresponds to three ligands, two coppers, four perchlorates and two methanol molecules. The fragmentation pattern shows the successive loss of one ligand unit, one perchlorate anion, the two methanol molecules and another perchlorate, followed by the two remaining perchlorates, the two copper ions and, finally, the second ligand to give one protonated ligand as the base peak. Therefore, it seems that the replacement of the terminal nitrogen complexation sites

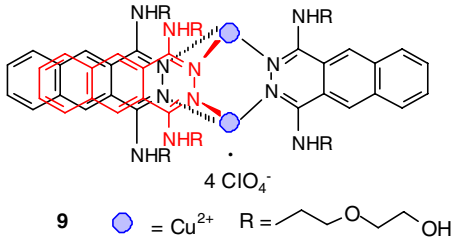

Figure 4.

by oxygen substantially modifies the nature of the complex formed. Unfortunately, **9** was not obtained as a solid, but as a jelly substance. The complex solidifies on standing in a vacuum desiccator but in contact with air becomes jelly again, probably due to fast coordination with water molecules. This fact prevented further study of its geometry by other techniques.

Due to the interest of confirming the crucial structural differences originated in complexation when the nitrogen sites at the end of the sidechains are replaced by oxygen, we decided to prepare the complex of ligand **3** with Zn(II), as both metals exhibit usually a similar behaviour in their complexation geometries. The addition of a methanol solution of anhydrous zinc chloride over a methanol solution of **3** originated the fast formation of a yellow precipitate of the complex **10** which was isolated as a stable solid with mp = 185–189 °C. Elemental analysis gave a molecular formula $C_{80}H_{106}O_{17}N_{16}Zn_2Cl_4$ tentatively fitting to $\{[Zn_2(L^3)_4]\text{-}Cl_4\cdot H_2O\}$.

The FAB mass spectrum of **10** exhibits a molecular peak with *m*/*z* = 1821, that is in accordance with the proposed formula after loss of the water molecule, and shows the initial and successive losses of four chloride ions, followed by one ligand unit, the two zinc atoms and, finally, two more ligands. The IR spectrum supports the coordination of the metallic ions with the pyridazine units, because the free ligand *ν*(CN) bands at 1508 and 1553 cm^{-1} are respectively shifted at 1554 and 1579 cm^{-1} in complex **10**.[17] However, the *ν*(CO) bands are not significantly modified, suggesting that the oxygen atoms are not participating. On the other hand, the wide and strong ligand *ν*(OH) band at 3315 cm^{-1} moves to 3357 cm^{-1} in **10**, with a shoulder ca. 3300 cm^{-1}, indicating strong hydrogen bonding of the lateral chains[24] instead of participation in complexation. Finally, a weak new band found in the far IR spectrum of the complex at 362 cm^{-1} should be assigned to the *ν*(ZnN) mode.[25]

The replacement of Cu(II) by Zn(II) allowed the inclusion of ^1H and ^{13}C NMR spectral data in structural considerations. When comparing the ^{13}C spectra of the podand **3** and its complex **10**, measured in DMSO-d_6, it is shown that the signals corresponding to the side-chain carbons neighbouring the OH group ($C_{3'}$ and $C_{4'}$) are practically unaffected by complexation ($\Delta\delta = 0.07$ and 0.09 ppm, respectively), whereas those ones of the two remaining methylenes and the aromatic $C_1$and C_4 exhibit more consistent variations ranging from 0.3 to 1.0 ppm. The same pattern is found in the comparison of the ^1H spectra, confirming that side chain oxygens are not taking part in complexation.

In consequence, it seems that the change in the nature of the donor sites at the sidechains causes a remarkable modification in the geometry of complexation and, as will be commented below, this fact could be responsible for differences in the biological activities of the podands.

Table 4. In vitro activity of 1,4-bis(alkylamino)benzo[*g*]phthalazines **1**–**3** on *Trypanosoma cruzi* epimastigotes

Compound	IC_{50} (μg/mL)			Toxicity IC_{50}[a] (μg/mL)
	24 h	48 h	72 h	
Benznidazole	—	—	4.12	3.53
1	56.75	12.85	3.25	6.25
2	n.d.	15.61	12.02	67.32
3	75.43	62.64	30.60	93.52

IC_{50}, concentration required to give 50% inhibition, calculated by linear regression analysis from K_c values at the concentrations employed (1, 10 and 25 μg/mL). n.d., not determined.
Note. Average of three separate determinations.
[a] On Vero cells at 72 h of culture.

3. Biological evaluation

In a first step, the effect of podands **1**–**3** on the in vitro growth of *T. cruzi* epimastigotes was measured, since we thought that the complexing ability of these compounds could support trypanocidal activity. In fact, very good inhibitory activity against the same parasite has been reported for quinone derivatives containing polyaminic chains related to those present in our compounds.[26] The growth inhibition of the parasite was measured at different times according to established procedures (see Section 4). Results obtained are displayed in Table 4 with benznidazole as the reference drug. The three compounds tested were active in this biological

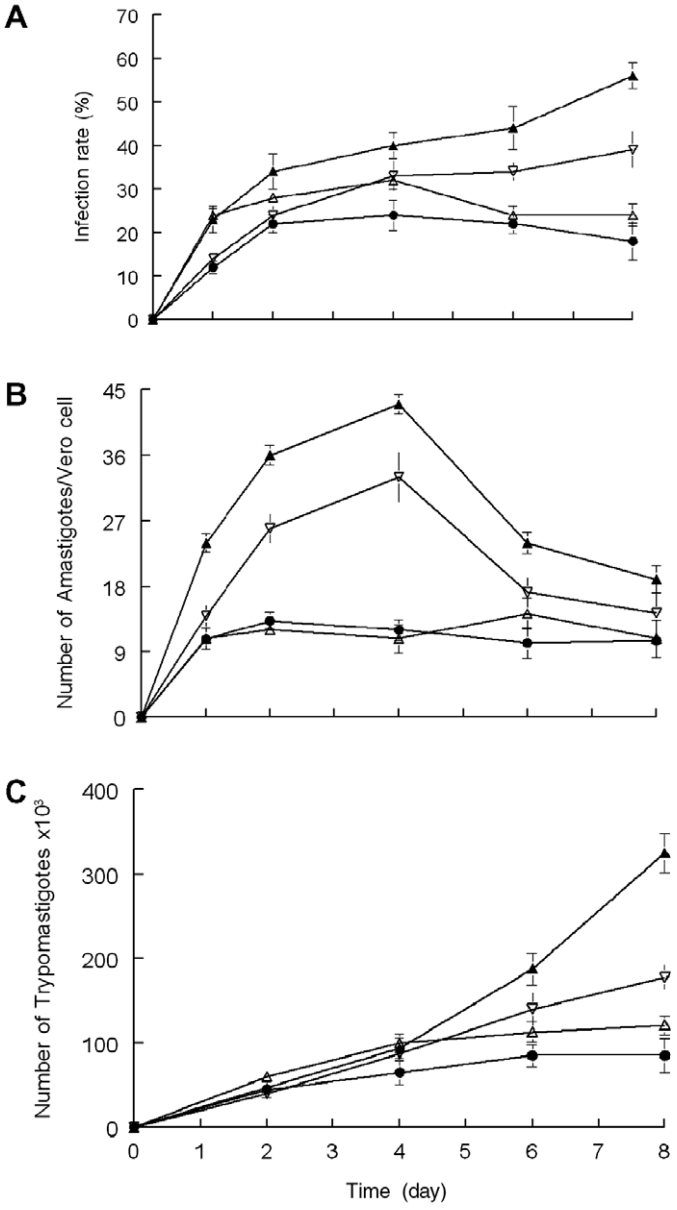

Figure 5. Effect of compounds **1**–**3** on the infection rate and *T. cruzi* growth. (A) rate of infection. (B) mean number of amastigotes per infected Vero cell. (C) number of trypomastigotes in the culture medium. Symbols: ▲, control; ▽, **1**; △, **2**; ●, **3** (at 5 μg/mL concn). The values are means of four separate experiments and the bars represent the standard deviation.

system. Compound **1** exhibited the highest toxicity against *T. cruzi* epimastigotes with IC_{50} values within the range of the reference drug. Compound **2** was also active, with lower potency than **1**. The antitrypanocidal activity observed for **2** was not associated to host cell toxicity (IC_{50} = 67.32 μg/mL). Compound **3** showed in all cases a remarkably lesser activity than **1** and **2**, and this fact could be related to the different mode of complexation of metal ions discussed above for that compound.

Figure 5 illustrates *T. cruzi* propagation in Vero cells (with and without co-addition of the test compounds). When 1×10^5 Vero cells were incubated for 2 days and then infected with 1×10^6 metacyclic forms, the parasites invaded the cells and underwent morphologic conversion to amastigotes within 1 day after infection. On days 1, 2, 4, 6 and 8, the rate of host-cell infection increased to 23%, 34%, 40%, 44%, and 56%, respectively. When compound **1** was simultaneously added to the infected Vero cells with *T. cruzi* metacyclic forms (5 μg/mL), the infection rate significantly decreased (35%) with respect to the control on day 2, reaching a 68% inhibition on day 8. Compound **2** at 5 μg/mL significantly inhibited the percentage of infected cells with a 57% inhibition on culture day 8 (Fig. 5A).

The average number of amastigotes per infected cell increased to 36 on day 2 and 43 on day 4, decreasing to 24 on day 6 and 19 on day 8, for the control experiment (Fig. 5B). Compounds **1** and **2** were highly inhibitory of *T. cruzi* amastigote replication in Vero cells in vitro (Fig. 5B) when simultaneously added to the cell culture infected with *T. cruzi* metacyclic forms. The addition of 5 μg/mL of **1** and **2** markedly lowered the amastigote number per infected cell to 12 and 10.8 on day 4 and 10.5 and 10.8 on day 8 (44% and 43% reduction in amastigote number with respect to the control for culture day 8, compounds **1** and **2**, respectively). The decrease in the average amastigote numbers on day 5 for the control experiment coincided with the increase in trypomastigote numbers in the medium (Fig. 5C). The number of trypomastigotes in the medium was 1×10^4 on day 2 and 3.25×10^6 on day 8. Compounds **1** and **2** gave, respectively, 74% and 65% reductions in trypomastigote numbers (Fig. 5C).

These results prompted us to evaluate the inhibitory effect of podands **1**–**3** on SOD activity, in order to test their potential as competitors for the metallic ions of the enzyme. We have used epimastigote forms from the Maracay strain of *T. cruzi* that excrete FeSOD when cultured in calf foetal serum.[27] Data obtained for the inhibition activity of the enzyme are displayed in Table 5.

Significant inhibition values of the enzyme activity ($p < 0.025$) are found for **1** and **2**. Podand **2** shows a 100% inhibition at a 25 μg/mL dosis, whereas **1** achieves 64% at 1 μg/mL. As in the previous test, the behaviour of **3** markedly differs from those ones of the other two podands, showing a much lesser activity against the parasitic SOD. All those results might be indicating that one of the action mechanisms of these compounds is blocking the metal ion of the enzyme, giving place to a substantial reduction of its activity.

Table 5. In vitro inhibition of Fe–SOD in *Trypanosoma cruzi* epimastigotes: 23.36 ± 4.21 U/mg

Compound	1 μg/mL	10 μg/mL	25 μg/mL
1	64**	68**	75**
2	48*	73**	100**
3	27	34*	53**

Values are the average of five separate determinations. Significant differences between the activities of the control homogenate and that one incubated with the tested compounds were obtained according to the Newman–Keuls test.
* $p < 0.05$.
** $p < 0.025$.

Table 6. Cu Zn–SOD activity inhibition (%) in human erythrocytes: 23.36 ± 4.21 U/mg

Compound	1 μg/mL	10 μg/mL	25 μg/mL
1	0	7	11
2	0	11	17
3	0	0	0

A high degree of activity against the SOD of the parasite should be nothing if the same pattern was found for human SOD without any discrimination. Therefore, we have also tested the effect of compounds **1**–**3** over CuZn-SOD belonging to human erythrocytes (Table 6).

Inhibition percentages at the higher dosages are very small in all cases for human SOD, and all the three compounds are fully inactive at the dosis of 1 μg/mL. These results enhance the potential antiparasitical interest of the alkylaminobenzo[*g*]phthalazine derivatives studied in this work.

In definitive, we have prepared a new series of compounds with complexing ability towards transition metal ions, that behave as SOD inhibitors and in which the mode of complexation could be related to the enzyme inhibition patterns and antiparasitical activity observed, although more work should be required in order to prove that relation.

4. Experimental

4.1. General

The starting compounds 2-(2-aminoethoxy)ethanol and 2-(2-aminoethoxy)ethylamine were purchased from Aldrich and used without further purification. 1,4-Dichlorobenzo[*g*]phthalazine was obtained from 2,3-naphthalenedicarboxylic acid following a method previously described.[28] All the reactions were monitored using thin layer chromatography (TLC) on precoated aluminium sheets of silica gel and compounds were detected with UV light (245 nm). Flash column chromatography was performed in the indicated solvent supported on silica

gel (particle size 0.040–0.063 mesh). Melting points were determined in Gallenkamp or Kofler apparatus and are uncorrected. ^{1}H NMR spectra were recorded at 300 MHz and ^{13}C NMR spectra at 75 MHz at room temperature employing CD_3OD and/or DMSO-d_6 as solvents. Chemical shifts are reported in ppm from TMS (δ scale). All assignments were performed on the basis of ^{1}H–^{13}C heteronuclear multiple quantum coherence experiments (gHSQC and gHMBC). Mass spectra were recorded by electronic impact (EI) at 70 eV, or by the fast atomic bombardment (FAB) technique with a VC Auto Spec spectrometer using a *m*-nitrobenzyl alcohol (NBA) matrix. EPR spectroscopy measurements were made at 300 and 120 K with a Bruker ER-200D spectrometer, equipped with variable temperature device. IR spectra were recorded on a Perkin-Elmer 597 spectrometer (4000–400 cm^{-1} range) and on an IR Bruker IFS 144C spectrometer (700–100 cm^{-1} range). Electronic spectra were recorded on a Perkin-Elmer Lambda 15 spectrometer, equipped with diffuse reflectance device, in the near infrared region, suspending the product in Nujol over filter paper. Magnetic susceptibility in range 4–100 K or 4–300 K was measured on a Squid magnetometer from Quantum Design equipped with helium cryostat. Magnetic susceptibility experimental values were corrected for diamagnetic contributions and TIP (temperature independent paramagnetism) was estimated as 100×10^{-8} emu mol^{-1} per Cu(II) ion.[28]

TGA/DTG analysis profiles (pyrolysis, 300–1000 K, with IR and MS investigation of evolved gases) were recorded under a 100 mL min^{-1} air flow using a Shidmazu TGA-DTG-50H Thermobalance coupled to a Nicolet Magma 550 FT-IR apparatus and a Fisons Thermolab mass spectrometer.

4.2. Synthesis of 3-(2-pyridilmethoxy)propylamine

To a stirred solution of 2-pyridilmethanol (6.0 g, 55 mmol) in anhydrous DME (150 mL) at 60 °C, an 80% suspension of sodium hydride in oil (1.65 g, 55 mmol) was added under argon. After 30 min, a solution of *N*-(3-bromopropyl)phthalimide (14.7 g, 57 mmol) in DME (100 mL) was added dropwise, the resulting mixture heated at 60 °C during 4 h and then stirred overnight at rt. After that, the reaction mass was treated with an aqueous 15% ammonium chloride solution until neutral pH. The aqueous phase was separated and extracted several times with chloroform. Evaporation of the solvent in the organic phase gave dark brown syrup that was flash column chromatographed using ethyl acetate/ethanol (10:1) as the eluent. The fraction of R_f 0.70 afforded 3.04 g (19%) of yellow oil. The so-obtained phthalimide was added over a 0.2 M hydrazine solution in methanol and the mixture was heated for 4 h at 40 °C. The solvent was removed under reduced pressure and the remaining white solid was purified by flash column chromatography ($CHCl_3$/EtOH/28% aqueous NH_4OH; 1:1:0.1) to give 0.82 g (50%) of the desired amine as an oil (R_f = 0.39). Anal. calcd for $C_9H_{14}N_2O$: C, 65.06; H, 8.43; N, 16.85. Found: C, 65.17; H, 8.62; N, 16.58; IR (KBr, cm^{-1}) 3400–3000, 3380, 3060, 2960, 2880, 1710, 1640, 1600, 1580, 1480, 1440, 1360, 1140, 1050, 670; ^{1}H NMR (CD_3OD): δ 8.48 (d, 1H, H-6′), 7.83 (t, 1H, H-4′), 7.50 (d, 1H, H-3′), 7.33 (m, 1H, H-5′), 4.59 (s, 2H, H-4), 4.44 (sa, 2H, NH_2), 3.64 (t, 2H, H-3), 2.83 (t, 2H, H-1), 1.85 (q, 2H, H-2); ^{13}C NMR (CD_3OD): δ 159.80 (C-2′), 149.88 (C-6′), 139.24 (C-4′), 124.48 (C-3′), 123.56 (C-5′), 74.41 (C-4), 70.44 (C-3), 40.19 (C-1), 32.83 (C-2); MS (FAB), *m*/*z* (%): 167 (MH^+, 1), 149 (2), 137 (1), 108 (90), 93 (100), 77 (8).

4.3. Synthesis of the 3-(2-pyridilmethoxy)propylamine derivatives 1 and 4

A solution of 1,4-dichlorobenzo[*g*]phthalazine (194 mg, 0.78 mmol) and 3-(2-pyridilmethoxy)-propylamine (520 mg, 3.13 mmol) in xylene (50 mL) was refluxed for 2 h. The reaction mixture was cooled to room temperature and the solvent removed under reduced pressure. The solid residue was purified by flash column chromatography (toluene/$CHCl_3$/EtOH, 2:1:1). The appropriate fractions (monitored by TLC) were combined to give two alkylamination products.

4.3.1. 1,4-Bis-[3-(2-pyridilmethoxy)propylamino]benzo-[*g*]phthalazine (1). The most retained fraction (R_f = 0.13) afforded an oil which was identified as the hydrochloride of **1**. The chromatographic treatment of that compound over basic aluminium oxide using chloroform as the eluent gave place to 100 mg (39%) of a yellow oil identified as the free polyamine **1**. Anal. calcd for $C_{30}H_{32}O_2N_6{\cdot}H_2O$: C, 68.44; H, 6.46; N, 15.96. Found: C, 68.56; H, 6.31; N, 15.83; IR ($CHCl_3$, cm^{-1}) 3600–3000, 1649, 1551; 1506, 1118, 1048; ^{1}H NMR (CD_3OD): δ 8.55 (s, 2H, H-5, H-10), 8.41 (d, 2H, H-6″), 7.98 (m, 2H, H-6, H-9), 7.71 (t, 2H, H-4″), 7.65 (m, 2H, H-7, H-8), 7.50 (d, 2H, H-3″), 7.23 (m, 2H, H-5″), 4.60 (s, 4H, H-4′), 3.75 (t, 4H, H-3′), 3.66 (m, 4H, H-1′), 2.12 (m, 4H, H-2′); ^{13}C NMR (CD_3OD): δ 159.62 (C-2″), 150.90 (C-1, C-4), 149.47 (C-6″), 138.82 (C-4″), 135.32 (C-5a, C-9a), 129.81 (C-6, C-9), 129.01 (C-7, C-8), 124.06 (C-3″), 123.45 (C-5, C-10), 123.32 (C-5″), 119.90 (C-4a, C-10a), 74.25 (C-4′), 70.66 (C-3′), 40.57 (C-1′), 30.14 (C-2′); MS (FAB), *m*/*z* (%): 509 (MH^+, 1), 399 (4), 277 (5), 263 (21), 210 (3), 91 (100).

4.3.2. 1-[3-(2-Pyridilmethoxy)propylamine]-4-chlorobenzo[*g*]phthalazine (4). The less retained fraction (R_f = 0.55) afforded 73 mg (25% yield) of **4** as a yellow oil. Anal. calcd for $C_{21}H_{19}ON_4Cl$: C, 66.58; H, 5.02; N, 14.79. Found: C, 66.50; H, 5.23; N, 14.99; IR (Cl_3CH, cm^{-1}) 3600–3000, 3340, 2950, 1635, 1580, 1440, 750; ^{1}H NMR (CD_3OD): δ 8.47 (s, 1H, H-10), 8.36 (s, 1H,H-5), 8.35 (d, 1H, H-6″), 7.96 (m, 1H), 7.87 (m,1H), 7.67 (t, 1H, H-4″), 7.59 (m, 2H, H-7,H-8), 7.43 (d, 1H, H-3″), 7.19 (t, 1H, H-5″), 4.55 (s, 2H, H-4′), 3.69 (t, 2H, H-3′), 3.67 (t, 2H, H-1′), 2.10 (m, 2H, H-2′); ^{13}C NMR (CD_3OD): δ 159.76 (C-2″), 155.59 (C-1), 149.80 (C-6″), 146.45 (C-4), 139.12 (C-4″), 136.09 (C-9a), 135.97 (C-5a), 130.31/130.28 (C-6/C-9), 130.14 (C-7, C-8), 126.81 (C-5), 124.46 (C-10), 124.39 (C-3″), 123.78 (C-4a), 123.61 (C-5″),

119.37 (C-10a), 74.54 (C-4′), 70.59 (C-3′), 40.92 (C-1′), 30.04 (C-2′); MS (IE) *m/z* (%): 379, (M^+, 83), 343 (2), 286 (80), 270 (100), 229 (19).

4.4. Synthesis of the 2-(2-aminoethoxy)ethylamine derivatives 2 and 5

A solution of 1,4-dichlorobenzo[*g*]phthalazine (100 mg, 0.40 mmol) and 2-(2-aminoethoxy)ethylamine (860 mg, 8.30 mmol) in xylene (50 mL) was refluxed for 1 h. The reaction mixture was cooled to room temperature and the solvent removed under reduced pressure. The solid residue was purified by flash column chromatography ($CHCl_3$/EtOH/28% aqueous NH_4OH, 1:1:0.2) to give the two alkylamination products.

4.4.1. 1,4-Bis-[2-(2-aminoethoxy)ethylamino]benzo[*g*]-phthalazine (2). The most retained fraction ($R_f = 0.54$) afforded 40 mg (26%) of **2** as a yellow solid with mp 60–63 °C. Anal. calcd for $C_{20}H_{28}O_2N_6 \cdot H_2O$: C, 59.70; H, 7.46; N, 20.79. Found: C, 59.11; H, 6.90; N, 19.92; IR (KBr, cm^{-1}) 3500–3300, 1631, 1551; 1506, 1114, 1032; ^1H NMR (CD_3OD): δ 8.59 (s, 2H, H-5, H-10), 8.05 (m, 2H, H-6, H-9), 7.62 (m, 2H, H-7, H-8), 3.81 (t, 4H, H-2′), 3.73 (t, 4H, H-3′), 3.56 (t, 4H, H-1′), 2.80 (t, 4H, H-4′); ^{13}C NMR (CD_3OD): δ 151.27 (C-1, C-4), 135.62 (C-5a, C-9a), 130.10 (C-6, C-9), 129.31 (C-7, C-8), 123.73 (C-5, C-10), 120.09 (C-4a, C-10a), 73.54 (C-3′), 70.82 (C-2′), 43.13 (C-1′), 42.84 (C-4′); MS (FAB), *m/z* (%): 385 (MH^+, 57), 342 (10), 298 (56), 279 (39), 211 (100).

4.4.2. 1-[2-(2-Aminoethoxy)ethylamino]-4-chlorobenzo-[*g*]phthalazine (5). The less retained fraction ($R_f = 0.65$) afforded 44 mg (35%) of **5** as a yellow oil. Anal. calcd for $C_{16}H_{17}ON_4Cl$: C, 57.40; H, 5.68; N, 16.74. Found: C, 57.26; H, 5.43; N, 16.51; IR (KBr, cm^{-1}) 3600–3100, 3050; 2920; 1629, 1560, 1430, 746; ^1H NMR (CD_3OD): δ 8.64 (s, 1H H-10), 8.48 (s, 1H, H-5), 8.05 (m, 2H, H-6, H-9), 7.66 (m, 2H, H-7, H-8), 3.81 (m, 4H, H-2′, H-3′), 3.58 (t, 2H, H-1′), 2.84 (t, 2H, H-4′); ^{13}C NMR (CD_3OD): δ 155.43 (C-1), 146.25 (C-4), 135.58 (C-9a), 135.36 (C-5a), 129.81 (C-6, C-9), 129.67 (C-7, C-8), 126.12 (C-5), 123.83 (C-10), 123.27 (C-4a), 118.83 (C-10a), 72.62 (C-3′), 70.00 (C-2′), 42.74 (C-1′), 42.00 (C-4′); MS (FAB), *m/z* (%): 317 (MH^+, 88), 289 (13), 274 (15), 256 (17), 229 (100).

4.5. Synthesis of the 2-(2-aminoethoxy)ethanol derivatives 3 and 6

A solution of 1,4-dichlorobenzo[*g*]phthalazine (284 mg, 1.14 mmol) and 2-(2-aminoethoxy) ethanol (1.75 g, 17.10 mmol) in xylene (50 mL) was refluxed for 1 h. The reaction mixture was cooled to room temperature and the solvent removed under reduced pressure. The residue was purified by flash column chromatography (chloroform/toluene/ethyl acetate/methanol, 1:1:2:3) to give the two alkylamination products.

4.5.1. 1,4-Bis[2-(2-hydroxyethoxy)ethylamino]benzo[*g*]-phthalazine (3). The most retained fraction ($R_f = 0.10$) afforded 115 mg (46%) of a yellow solid with mp 129–132 °C. Anal. calcd for $C_{20}H_{26}N_4\ O_4 \cdot H_2O$: C, 59.40; N, 13.86; H, 6.43. Found: C, 60.10; N, 14.04; H, 6.74; IR (KBr, cm^{-1}) 3500–3000, 3315, 1629, 1553, 1508, 1123; ^1H NMR (CD_3OD): δ 8.59 (s, 2H, H-5, H-10), 8.05 (m, 2H, H-6, H-9), 7.61 (m, 2H, H-7, H-8), 3.83 (t, 4H, H-4′), 3.72 (t, 8H, H-2′, H-3′), 3.63 (t, 4H, H-1′); ^1H NMR (DMSO-d_6): δ 8.82 (s, 2H, H-5, H-10), 8.11 (m, 2H, H-6, H-9), 7.70 (m, 2H, H-7, H-8), 3.67 (s, 4H, H-4′), 3.64 (t, 4H, H-3′), 3.50 (m, 4H, H-2′), 3.34 (t, 4H, H-1′); ^{13}C NMR (CD_3OD): δ 151.34 (C-1, C-4), 135.61 (C-5a, C-9a), 130.10 (C-6, C-9), 129.32 (C-7, C-8), 123.79 (C-5, C-10), 120.04 (C-4a, C-10a), 73.78 (C-3′), 70.93 (C-2′), 62.55 (C-4′), 43.18 (C-1′); ^{13}C NMR (DMSO-d_6): δ 148.60 (C-1, C-4), 133.17, 128.56, 127.71, 122.22, 118.00 (C aromat.), 72.16 (C-3′), 68.90 (C-2′), 60.20 (C-4′), 41.12 (C-1′); MS (FAB), *m/z* (%): 387 (MH^+, 14), 386 (M^+, 21), 355 (6), 298 (56), 253 (8), 210 (100).

4.5.2. 1-[2-(2-Hydroxyethoxy)ethylamino]-4-chlorobenzo[*g*]-phthalazine (6). The less retained fraction ($R_f = 0.78$) afforded 133 mg (36%) of a yellow solid with mp 136–138 °C. Anal. calcd for $C_{16}H_{16}N_3\ O_2Cl \cdot H_2O$: C, 57.23; H, 5.36; N, 12.52; Cl, 10.00. Found: C, 57.41; H, 5.24; N, 12.38; Cl, 10.78; IR (Cl_3CH, cm^{-1}) 3500–3000, 1520, 1450, 1370, 1300; ^1H NMR (CD_3OD): δ 8.46 (s, 1H, H-10), 8.28 (s, 1H, H-5), 7.91 (m, 2H, H-6, H-9), 7.58 (m, 2H, H-7, H-8), 3.83 (t, 2H, H-4′), 3.77 (t, 2H, H-3″), 3.73 (t, 2H, H-2′), 3.65 (t, 2H, H-1′); ^{13}C NMR (CD_3OD): δ 155.93 (C-1), 146.81 (C-4), 136.16 (C-9a), 135.99 (C-5a), 130.36 (C-6, C-9), 130.24 (C-7, C-8), 126.74 (C-5), 124.54 (C-10), 123.86 (C-4a), 119.39 (C-10a), 74.00 (C-3′), 70.54 (C-2′), 62.73 (C-4′), 43.37 (C-1′); MS (FAB), *m/z* (%): 319 (MH^+, 5), 272 (10), 256 (12), 229 (100).

4.6. Synthesis of the Cu(II) dinuclear complexes

4.6.1. General method. A solution of 0.30 mmol of copper(II) perchlorate hexahydrate in dry methanol (2 mL) was added dropwise over a solution of the corresponding ligand (0.15 mmol) in 2 mL of the same solvent. A green precipitate slowly appeared during the addition. After 30 min stirring at rt, the solid complex was separated by centrifugation and exhaustively dried by heating under vacuum.

4.6.2. Complex 7 $\{[Cu_2L^1](OH)_2\ (ClO_4)_2 \cdot CH_3OH\}$. Yield 100 mg, 74%. Mp 200–205 °C. Anal. calcd for $C_{31}H_{38}Cl_2\ Cu_2N_6O_{13}$: C, 41.33; H, 4.22; N, 9.33; Cl, 7.88. Found: C, 41.82; H, 4.37; N, 9.79; Cl, 7.92; IR (KBr, cm^{-1}) 3400, 3280, 1551, 1506, 1144, 1121, 1109, 1086, 626; MS (FAB), *m/z* (%): 901 (MH^+, 0.01), 870 (0.5), 771 (0.5), 735 (4.5), 671 (4), 635 (4), 571 (82), 509 (L^1H^+, 100).

4.6.3. Complex 8 $\{[Cu_2L^2](OH)(ClO_4)_3 \cdot 2H_2O\}$. Yield 54 mg, 39%. Mp > 300 °C. Anal. calcd for $C_{20}H_{33}Cl_3\ Cu_2N_6O_{17}$: C, 27.74; H, 3.81; N, 9.71, Cl, 12.31. Found: C, 27.61; H, 3.63; N, 9.40, Cl, 12.08; IR (KBr, cm^{-1}) 3526, 3403, 3315, 3226, 1651, 1627, 1578, 1551, 1120, 1108, 1088, 940, 636, 626, 392, 324; MS (FAB), *m/z* (%): 865 (MH^+, 0.1), 765 (0.2), 665 (1.5), 611 (1.5), 447 (5.5), 385 (L^2H^+, 100).

4.6.4. Complex 9 {[$Cu_2(L^3)_3$] $(ClO_4)_4 \cdot 2CH_3OH$}. A careful concentration of the reaction mixture to half volume, followed by refrigeration during 24 h, and further centrifugation yielded 45 mg (10%) of the brilliant green complex. Anal. calcd for $C_{62}H_{86}Cl_4\ Cu_2N_{12}O_{30}$: C, 42.58; H, 4.92; N, 9.61, Cl, 8.12. Found: C, 42.27; H, 4.98; N, 9.18, Cl, 8.59; IR (KBr, cm^{-1}) 3600–3100, 3320, 1630, 1350, 1110, 900, 760, 630; MS (FAB), *m/z* (%): 1748 (MH^+, 0.1), 1362 (0.1), 1263 (8), 1099 (0.5), 999 (2.5), 898 (2), 837 (0.8), 773 (7), 387 (L^3H^+, 100).

4.7. Synthesis of the Zn(II) dinuclear complex 10 {$[Zn_2L^3{}_4]Cl_4 \cdot H_2O$}

A solution of 0.36 mmol of anhydrous zinc(II) chloride in methanol (2.5 mL) was added dropwise over a solution of the corresponding ligand (0.18 mmol) in methanol (2 mL). After 30 min stirring at rt, the solid complex was separated by filtration and exhaustively dried by heating under vacuum. Yield 80 mg, 21%. Mp 185–189 °C. Anal. calcd for $C_{80}H_{106}O_{17}\ N_{16}Zn_2Cl_4$: C, 52.32; H, 5.82; N, 12.20; Cl, 7.72. Found: C, 51.84; H, 5.81; N, 12.41; Cl, 7.45; IR (KBr, cm^{-1}) 3357, 1628, 1579, 1132, 1102, 1032, 362, 293, 283, 181, 136; ^1H NMR (DMSO-d_6): δ 8.97 (s, 2H, H-5, H-10), 8.22 (m, 2H, H-6, H-9), 7.84 (m, 2H, H-7, H-8), 3.85 (s, 4H, H-4′), 3.76 (t, 4H, H-2′), 3.72 (m, 4H, H-3′), 3.65 (t, 4H, H-1′); ^{13}C NMR (DMSO-d_6): δ 148.28 (C-1, C-4), 133.80, 129.72, 128.82, 125.24, 117.62 (C aromat.), 72.23 (C-3′), 67.84 (C-2′), 60.11 (C-4′), 41.70 (C-1′); MS (FAB), *m/z* (%): 1821 ($MH^+ - H_2O$ (0.1), 1749 (0.1), 1719 (0.2), 1672 (0.1), 1295 (0.2), 1223 (0.3), 1160 (0.1), 773 (7), 387 (L^3H^+, 100).

4.8. Biological Tests

4.8.1. Parasite strain, culture and trypanocidal in vitro studies. The Maracay strain of *T. cruzi* was isolated from a clinical specimen at the Institute of Malariology and Environmental Health in Maracay (Venezuela). Epimastigotes were cultivated in liquid Trypanosoma medium (MTL) supplemented with 10% inactivated foetal calf serum (IFCS, Sebak) at 28 °C. To obtain the parasite suspension for the trypanocidal assay, the epimastigote culture (in exponential growth phase) was concentrated by centrifugation at 1500 rpm for 10 min and the number of flagellates were counted in an haemocytometric chamber and distributed into aliquots of 2×10^6 parasites/mL.

The compounds were dissolved in methanol (Panreac, Barcelona, Spain) at a concentration of 1%, after assayed as non-toxic and without inhibitory effects on the parasite growth. The compounds were dissolved in the culture medium, and the dosages used were the following: 25, 10, and 1 μg/mL. The effect of each compound against epimastigote forms, as well as the concentrations, was evaluated at 24, 48 and 72 h, using a Neubauer haemocytometric chamber.

4.8.2. Cell culture and cytotoxicity tests. Vero cells (Flow) were grown in minimal essential medium (MEM) (Gibco) supplemented with 10% IFCS and adjusted to pH 7.2, in a humidified 95% air–5% CO_2 atmosphere at 37 °C for 2 days. In the test for cytotoxicity, cells were placed in 25 mL cone-based bottles (Steriling) and centrifuged at 1500 rpm for 5 min. The culture medium was removed, and fresh medium was added to a final concentration of 1×10^5 cells/mL. This cell suspension was distributed in a culture tray (with 24 wells) at a rate of 100 μL per well, and incubated for 2 days at 37 °C in humid atmosphere enriched with 5% CO_2. The medium was removed, and the fresh medium was added together with the product to be studied (at concentrations of 25, 10 and 1 μg/mL). The cultures were incubated for 72 h. The vital stain Trypan blue (0.1% in phosphate buffer) was used to determine cell viability. The number of dead cells was recorded, the percent viability calculated in comparison to that of the control culture, and the IC_{50} obtained by linear regression analysis from the K_c values at the employed concentrations.

4.8.3. Transformation of epimastigotes to metacyclic forms. To induce metacyclogenesis, parasites were cultured at 28 °C in modified Grace's medium (Gibco) for 12 days according to the methods described by Osuna et al.[29] Twelve days after cultivation at 28 °C, metacyclic forms were counted in order to infect Vero cells. The proportion of metacyclic forms was around 40% at this stage.

4.8.4. Amastigote-Vero cells assay. The experimental procedure was started with Vero cells maintained in MEM in a humidified 95% air–5% CO_2 atmosphere at 37 °C. Cells were seeded at a density of 1×10^5 cells/well in 24-well microplates (NUNC) with rounded coverslips on the bottom and cultivated for 2 days.

Vero cells cultured as above were infected in vitro with *T. cruzi* metacyclic forms at a ratio of 10:1. The drugs (5 μg/mL concentrations) were added immediately after infection and were incubated for 3 h at 37 °C in a 5% CO_2. The non-phagocytosed parasites and the drugs were removed by washing and then the infected cultures were grown for 8 days in fresh medium. Fresh culture medium was added every 48 h.

In all cases, the drug activity was determined from the percentage of infected cells and number of amastigotes per Vero cell infected in treated and untreated cultures in methanol-fixed and Giemsa-stained preparations. The percentage of infected Vero cells and the mean number of amastigotes per infected cell were determined by analysing more than 100 host cells distributed in randomly chosen microscopic fields. Values are means of four separate determinations. The number of trypomastigotes in the medium was determined as described previously.[30]

4.8.5. SOD enzymatic inhibition by the alkylaminobenzo[*g*]phthalazines 1, 2 and 3. The parasites cultured as described above were suspended (0.5–0.6 g wt mL^{-1}) in 3 mL of buffer 1 (0.25 M sucrose, 25 mM Tris–HCl, 1 M EDTA, pH 7.8) and disrupted by 3 cycles of sonic disintegration, 30 s each at 60 V. The sonicated

homogenate was centrifuged at 1500*g* for 10 min at 4 °C, and the pellet was washed three times with ice-cold STE buffer 1, for a total supernatant fraction of 9 mL. This fraction was centrifuged (2500*g* for 10 min at 4 °C), the supernatant collected and solid ammonium sulfate added. The protein fraction, which precipitated between 35% and 85% salt concentration, was centrifuged (9000*g* for 20 min at 4 °C), redissolved in 2.5 mL of 20 mM potassium phosphate buffer (pH 7.8) containing 1 mM EDTA (buffer 2) and dialysed in a Sephadex G-25 column (Pharmacia, PD 10), previously balanced with buffer 2, bringing it to a final volume of 3.5 mL (fraction of the homogenate).[31] The protein concentrations were determined by the Bradford method.

Iron superoxide dismutase (Fe–SOD) activity was determined by NAD(P)H oxidation according to Paoletti and Mocali.[32] One unit was the amount of enzyme required to inhibit the rate of NAD(P)H reduction by 50%. CuZnSOD from human erythrocytes used in these assays was obtained from Boehringer (Mannheim), while all the coenzymes and substrates came from Sigma Chemical Co. Data obtained were analysed according to the Newman–Keuls test.

Acknowledgments

The authors thank the Spanish Comision Interministerial de Ciencia y Tecnologia for the economical support given to this work (SAF99-0066). We are also grateful to the contribution of the Centro de Resonancia Magnetica Nuclear and the Centro de Microanalisis of the Univ. Complutense.

References and notes

1. Pez, D.; Leal, I.; Zuccotto, F.; Boussard, C.; Brun, R.; Croft, S.; Yardley, V.; Ruiz-Perez, L. M.; Gonzalez-Pacanowska, D.; Gilbert, I. H. *Bioorg. Med. Chem.* **2003**, *11*, 4693.
2. Zou, Y.; Wu, Z.; Sirisoma, N.; Woster, P. M.; Casero, R. A.; Weiss, L. M.; Rattendi, D.; Lane, S.; Bacchi, C. J. *Bioorg. Med. Chem. Lett.* **2001**, *11*, 1613.
3. Urbina, J. A.; Docampo, R. *Trends Parasitol.* **2003**, *19*, 495.
4. Cerecetto, H.; Gonzalez, M. *Curr. Top. Med. Chem.* **2002**, *2*, 1185.
5. Ghosh, S.; Goswami, S.; Adhya, S. *Biochem. J.* **2003**, *369*, 447.
6. Quesada, J. M.; Entrala, E.; Fernández-Ramos, C.; Marin, C.; Sánchez-Moreno, M. *Mol. Biochem. Parasitol.* **2001**, *115*, 123.
7. Fridovich, I. *Annu. Rev. Biochem.* **1995**, *64*, 64.
8. Casanova, C.; Alzuet, G.; Ferrer, S.; Latorre, J.; Ramírez, J. A.; Borras, J. *Inorg. Chim. Acta* **2000**, *304*, 170.
9. Vallet, M.; Faus, J.; Garcia-España, E.; Moratal, J.; *Introducción a la Química Bioinorganica*, *Parte III*; Ed. Síntesis (Madrid), **2003**, 228.
10. Siwik, D.; Tzortzis, J.; Pimental, D. R.; Chang, D.; Pagano, P. J.; Singh, K.; Sawyer, D. B.; Colucci, W. S. *Circ. Res.* **1999**, *85*, 147.
11. (a) Campayo, L.; Navarro, P. *Eur. J. Med. Chem.* **1986**, *21*, 143; (b) Campayo, L.; Cano, F. H.; Foces-Foces, C.; Navarro, P. *J. Chem. Soc. Perkin Trans. 2* **1987**, 569.
12. (a) Körmendy, K. *Acta Chim. Hung.* **1977**, *94*, 373; (b) Körmendy, K. *Acta Chim. Hung.* **1978**, *98*, 303.
13. Rodriguez-Ciria, M.; Sanz, A. M.; Yunta, M. J. R.; Gomez-Contreras, F.; Navarro, P.; Fernandez, I.; Pardo, M.; Cano, C. *Bioorg. Med. Chem.* **2003**, *11*, 2143.
14. Lever, A. B. P. *Inorganic Electronic Spectroscopy*; Elsevier: Amsterdam, 1984.
15. (a)*ESR and NMR of Paramagnetic Species in Biological and Related Systems*; Bertini, I., Drago, S. R., Eds.; Reidel Pub.: London, 1979; (b) Sorrel, T. N. *Tetrahedron* **1989**, *45*, 1; (c) Hathaway, B. J.. In *Comprehensive Coordination Chemistry*; Wilkinson, G., Gillard, J. A., Eds.; Mac Cleverty Ed.: Penguin, Oxford, 1987; Vol. 5, p 656, Chapter 53.
16. (a) Hathaway, B. J.; Underhill, A. E. *J. Chem. Soc.* **1964**, 3091; (b) Thompson, L. K.; Hartstock, F. W.; Rosemberg, L.; Woon, T. C. *Inorg. Chim. Acta* **1985**, 1; (c) Rosenthal, M. R. *J. Chem. Ed.* **1973**, *50*, 331.
17. Nakamoto, K. *Infrared and Raman Spectra of Inorganic and Coordination Compounds*; John Wiley: New York, 1997.
18. (a) Adams, D. M. *Metal Ligands and Related Vibrations*; E. Arnold: London, 1967; (b) Weidlein, J.; Müller, U.; Dehnicke, K. *Schwingungsfrequenzen II*; Verlag: Stuttgart, 1986.
19. (a) Kahn, O. *Molecular Magnetism*; VCH: Weinheim, 1993; (b) Hodgson, D. J. *Prog. Inorg. Chem.* **1975**, *19*, 173; (c) Sorrel, T. N.; Jameson, D. L.; Malachowski, D. L. *Inorg. Chem.* **1982**, *21*, 3250; (d) Gupta, R.; Gosh, D.; Mukherjee, R. *Proc. Indian Acad. Sci.* **2000**, *112*, 179; (e) Grillo, V. A.; Hambley, T. W.; Gahan, L. R.; Hanson, G. R.; Stranger, R.; Moubaraki, B.; Murray, K. S. *Aus. J. Chem.* **1999**, *52*, 861.
20. (a) Ghosh, D.; Mukherjee, R. *Inorg. Chem.* **1998**, *37*, 6597; (b) Morooka, Y.; Fujisawa, K.; Kitajima, N. *Pure Appl. Chem.* **1995**, *67*, 241; (c) Tapan, K.; Ghosh, K.; Mukherjee, R.; Ghosh, S. *Chem. Commun.* **1996**, 13.
21. (a) Berends, H. P.; Stephan, D. W. *Inorg. Chem.* **1987**, *26*, 749; (b) Evans, D. A.; Burgey, C. S.; Paras, N. A.; Vojkovsky, T.; Tregay, S. *J. Am. Chem. Soc.* **1998**, *120*, 5824; (c) Casella, L.; Carugo, O.; Gullotti, M.; Garofani, S.; Zanello, P. *Inorg. Chem.* **1993**, *32*, 2056.
22. Solomon, E. I. *Copper Proteins*, In Spiro, T. G. Ed.; John Wiley: New York, 1981; 41.
23. Maekawa, M.; Munakata, M.; Kuroda-Sowa, T.; Nozaka, Y. *J. Chem. Soc. Dalton Trans.* **1994**, 603.
24. Kumar, P. A.; Swathi, P.; Pisipati, V. G. K. M.; Rajeswari, A. V. *Cryst. Res. Technol.* **2002**, *37*, 595.
25. Castiñeiras, A.; Diaz, G.; Florencio, F.; Garcia-Blanco, S.; Martinez-Carrera, S. *Z. Anorg. Allg. Chem.* **1988**, *567*, 101.
26. Salmon-Chemin, L.; Lemaire, A.; De Freitas, S.; Deprez, B.; Sergheraert, C.; Davioud-Charvet, E. *Bioorg. Med. Chem. Lett.* **2000**, *10*, 631.
27. Villagran, M. E.; Marin, C.; Rodríguez-Gonzalez, I.; De Diego, J. A.; Sánchez-Moreno, M. *Am. J. Trop. Med. Hyg.* **2005**, *73*, 510.
28. (a) Earnshaw, A. *Introduction to Magnetochemistry*; Academic Press: London, 1968; (b) Orchard, A. F. *Magnetochemistry*; Oxford University Press: New York, 2003.
29. Osuna, A.; Adroher, F. J.; Lupiañez, J. A. *Cell Diff. Dev.* **1990**, *30*, 89.
30. Nakajima-Shimada, J.; Hirota, Y.; Auki, T. *Antimicrob. Agents Chemother.* **1996**, *40*, 2455.
31. Marín, C.; Hitos, A. B.; Rodríguez-Gonzalez, I.; Dollet, M.; Sánchez-Moreno, M. *FEMS Microbiol. Lett.* **2004**, *234*, 69.
32. Paoletti, F.; Mocali, A. *Methods Enzymol.* **1990**, *186*, 209.